

# Floquet prethermalization of lattice gauge theories on superconducting qubits

Tomoya Hayata  
Keio University

Collaborators: Yoshimasa Hidaka (YITP), Yuta Kikuchi (Quantinuum),  
Kazuhiro Seki (RIKEN), Arata Yamamoto (U. Tokyo), Seiji Yunoki (RIKEN)

References:

Kazuhiro Seki, Yuta Kikuchi, Tomoya Hayata, Seiji Yunoki, arXiv: 2405.07613 [quant-ph]

Tomoya Hayata, Kazuhiro Seki, Arata Yamamoto, arXiv:2408.10079 [hep-lat]

Tomoya Hayata, Yoshimasa Hidaka, arXiv: 2409.20263 [hep-lat]

# Table of contents

○ Why QC? → QC of QCD

○ q-deformed Yang-Mills theory (Easy examples:  $SU(2)_1$  and  $SU(3)_1$ )

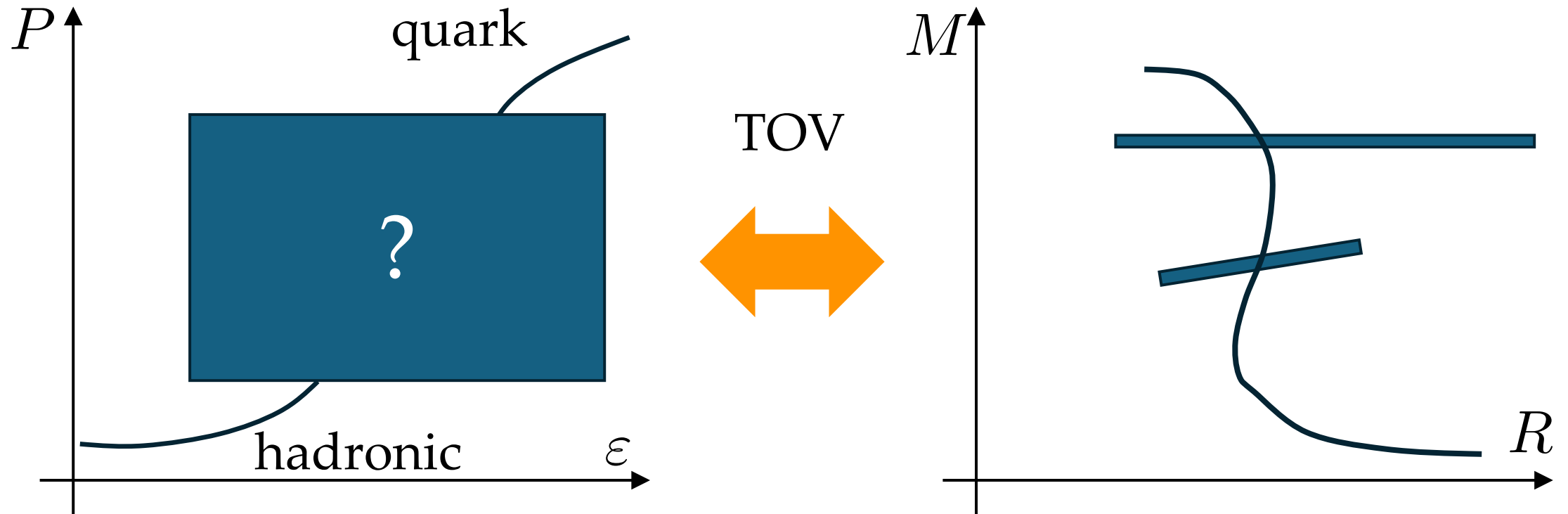
○ Why Floquet systems?

○ Experimental results

○ Summary

# Dense QCD and Neutron stars

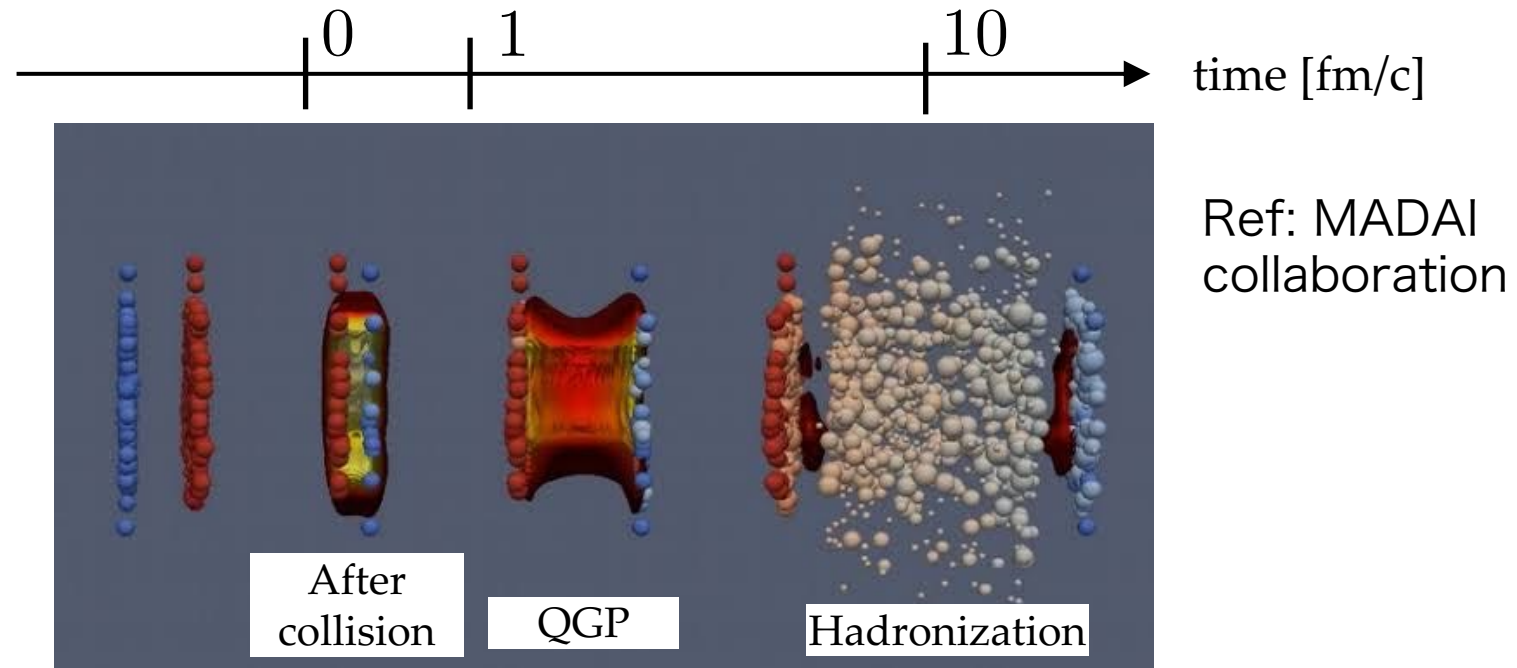
- Equation of state of QCD is relevant to astrophysics



Ground state “energy” of QCD as a function of the baryon number density

# Nonequilibrium QCD and Little bang

- Understand the dynamics of quark-gluon-plasma (QGP) created in heavy-ion collision experiments



Ab initio calculations of real-time QCD



# Two directions

○ Implementing QCD on quantum devices is never trivial

➔ Develop quantum algorithms and wait fault-tolerant QCs

➔ Simulating toy models of LGTs on NISQ devices

e.g., Schwinger model (QED in 1+1 dimensions )

# Table of contents

○ Why QC? → QC of QFT

○ q-deformed Yang-Mills theory (Easy examples:  $SU(2)_1$  and  $SU(3)_1$ )

○ Why Floquet systems?

○ Experimental results

○ Summary

# SU(N)<sub>k</sub> and graph representation

○ Wilson line (generates computational basis)

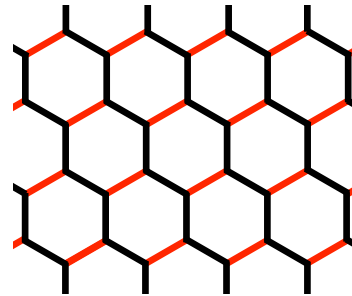
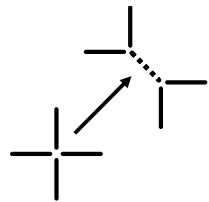
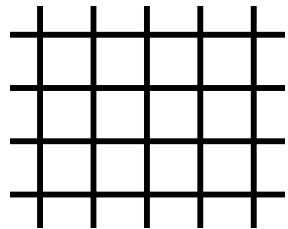
$d_a$  quantum dimension

$$\sqrt{d_a} U_a = \begin{array}{c} | \\ \hline \uparrow a \\ \hline | \end{array}$$

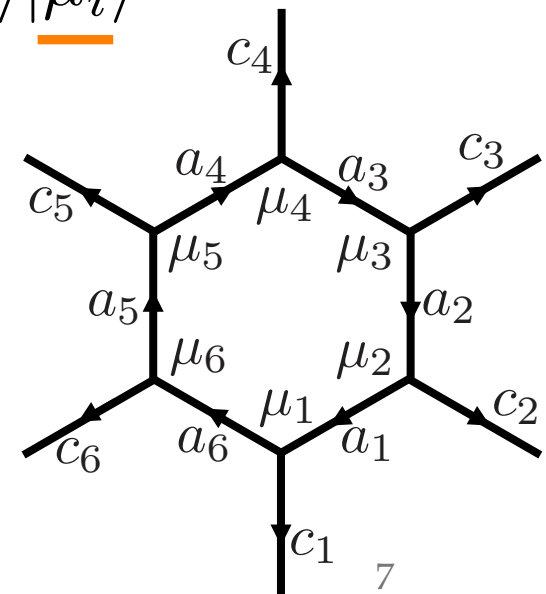
$a = (p_a, q_a, \dots)$  Dynkin index

multiplicity

○ 2d square lattice to state (2+1d Yang-Mills)



$$\prod_{i=1}^6 |a_i\rangle |c_i\rangle |\mu_i\rangle =$$



• Gauss's laws on vertices



Fusion rules

$$a \times b = \sum_c N_{ab}^c c$$

# SU(N)<sub>k</sub> and graph representation

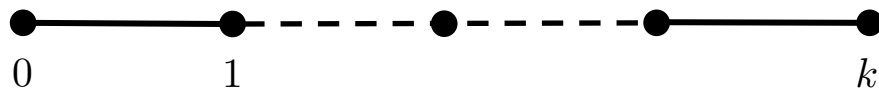
○ Wilson line (generates computational basis)

$d_a$  quantum dimension

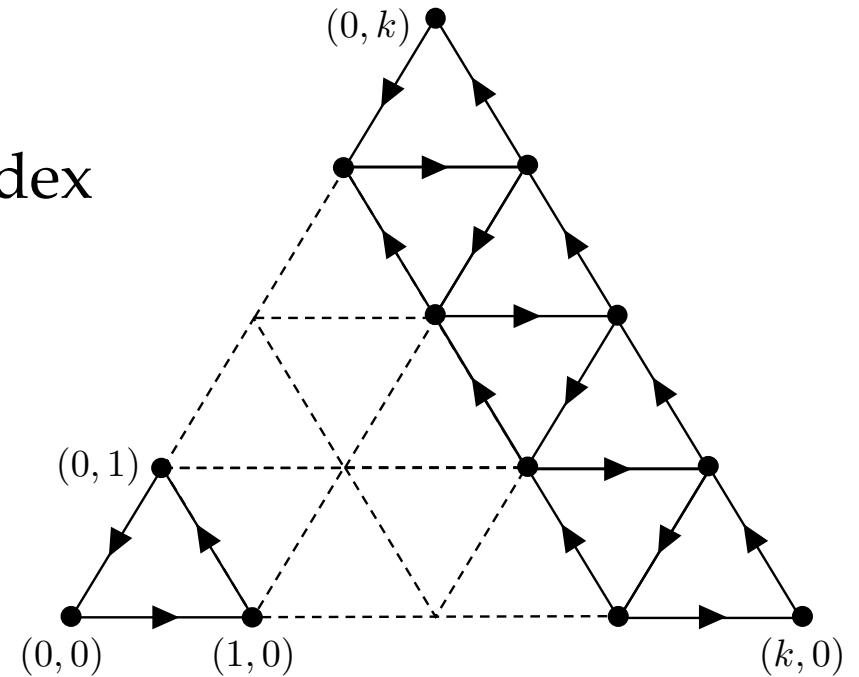
$$\sqrt{d_a} U_a = \begin{array}{c} | \\ \hline \uparrow \\ a \end{array}$$

$a = (p_a, q_a, \dots)$  Dynkin index

○ SU(2)<sub>k</sub>, SU(3)<sub>k</sub>, ...



$$\begin{aligned} (d+1)\text{-SU}(2)_k &= (d+1+1)\text{-spin}\frac{1}{2} \\ &= (d+1)\text{-qudit} \end{aligned}$$



$$(d+1)\text{-SU}(3)_k = (d+1+2)\text{-spin}\frac{1}{2}$$

$k$  is the length of “extra” dimensions

# SU(N)<sub>k</sub> and graph representation

○ Wilson line (generates computational basis)

$d_a$  quantum dimension

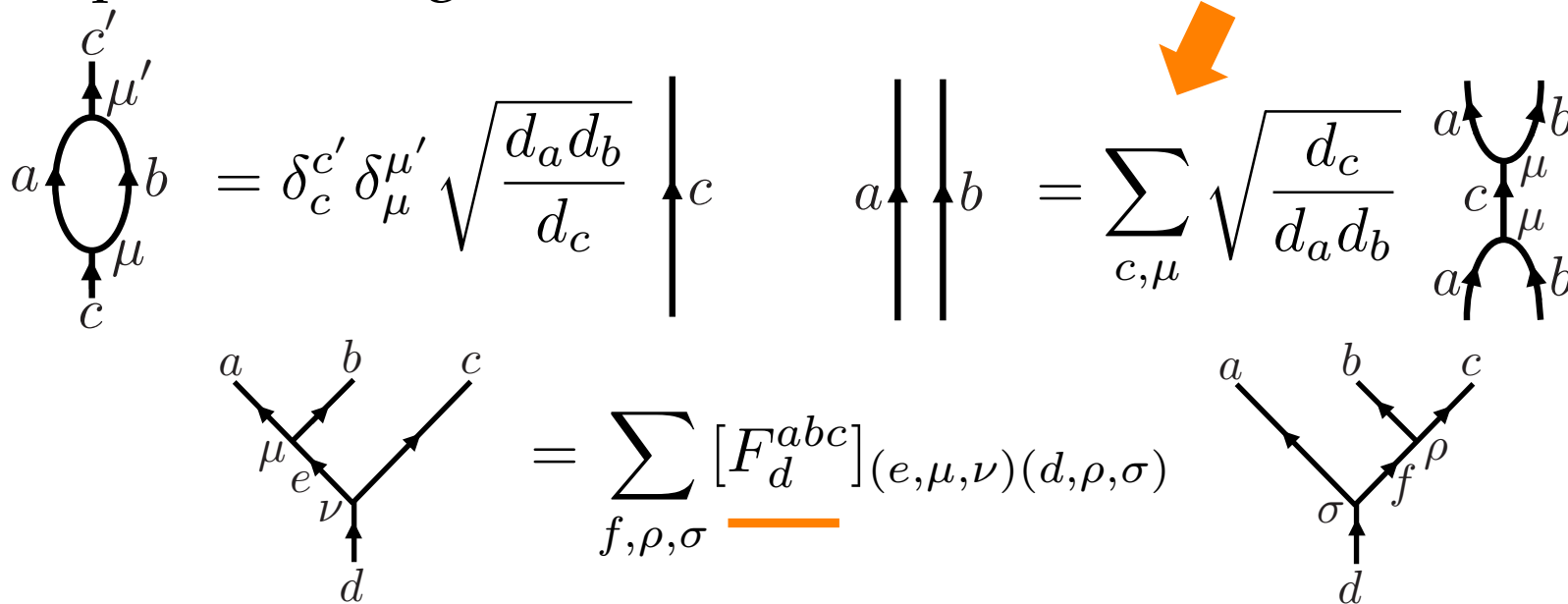
$$\sqrt{d_a} U_a = \left| \begin{array}{c} \uparrow \\ a \end{array} \right.$$

$a = (p_a, q_a, \dots)$  Dynkin index

Fusion rules

$$a \times b = \sum_c \underline{N_{ab}^c} c$$

○ Three important things



# q-deformed Yang-Mills theory

Zache, González-Cuadra, Zoller, PRL 131, 171902 (2023)  
 TH, Hidaka, JHEP 2023, 126 (2023); JHEP 2023, 123 (2023)

○ Kogut-Susskind Hamiltonian

$$H = \sum_{\mathbf{x}, \mu} \frac{1}{2} E^{a2}(\mathbf{x}, \mu) - \frac{K}{2} \sum_{p \in P} (\text{tr} U_p + \text{tr} U_p^\dagger)$$

○ q-deformed representation

$$K = 1/g^4$$

$$\begin{array}{c}
 (E^a(x, \mu))^2 \uparrow a = C_2(a) \uparrow a \\
 \\
 \text{tr} U_d \quad \begin{array}{c} \text{Diagram 1} \end{array} = \sum_{\{a'_i, \mu'_i\}} \prod_{i=1}^6 [F_{a'_i}^{c_i a_{i-1} d}]_{(a_i, \mu_i, \mu'_{i+1}), (a'_{i-1}, \mu'_{i-1}, \mu'_i)} \quad \begin{array}{c} \text{Diagram 2} \end{array}
 \end{array}$$

The diagram shows the q-deformed representation of the Kogut-Susskind Hamiltonian. It features a central equation:  $(E^a(x, \mu))^2 \uparrow a = C_2(a) \uparrow a$ . Below this, the trace of the deformed plaquette operator,  $\text{tr} U_d$ , is equated to a sum over configurations  $\{a'_i, \mu'_i\}$  of a product of six  $F$ -symbols. The  $F$ -symbols are  $[F_{a'_i}^{c_i a_{i-1} d}]_{(a_i, \mu_i, \mu'_{i+1}), (a'_{i-1}, \mu'_{i-1}, \mu'_i)}$ . Two diagrams illustrate the structure of the plaquette operator. The left diagram shows a hexagonal plaquette with vertices labeled  $\mu_1$  through  $\mu_6$  and edges labeled  $a_1$  through  $a_6$ . External edges are labeled  $c_1$  through  $c_6$ . The right diagram shows a similar hexagonal plaquette with vertices labeled  $\mu'_1$  through  $\mu'_6$  and edges labeled  $a'_1$  through  $a'_6$ . External edges are labeled  $c_1$  through  $c_6$ .

# Wilson loop (matrix elements)

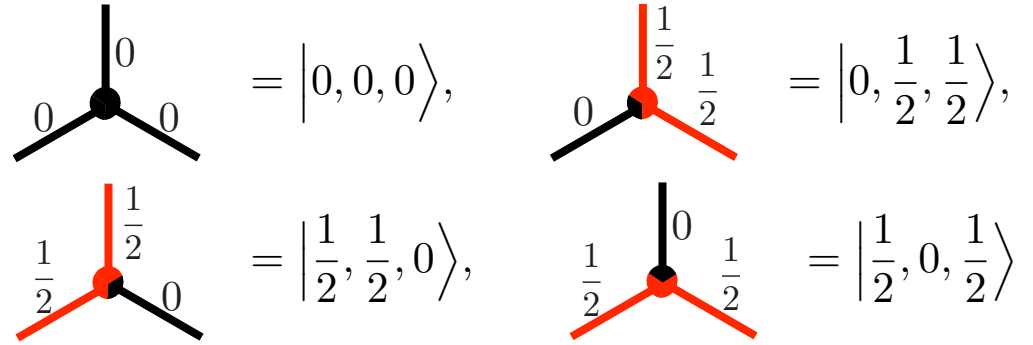
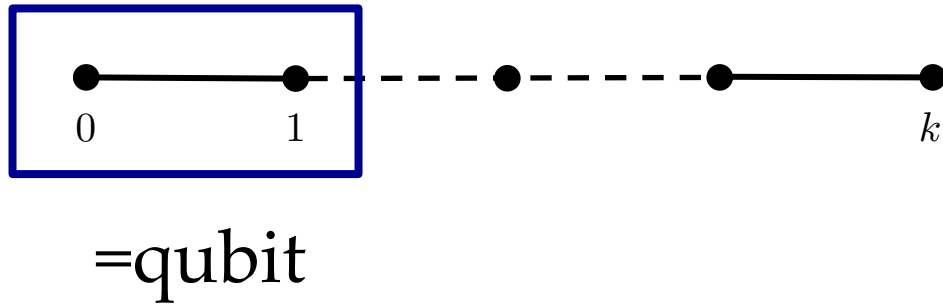
Robson, Webber, Z. Phys. C 15, 199 (1982)  
 Levin, Wen, PRB 71 045110 (2005)

$$\begin{aligned}
 & \text{Diagram 1: A square with vertices labeled } c_1, c_2, c_3, c_4 \text{ and edges labeled } a_1, a_2, a_3, a_4. \text{ A circle with a cross inside is labeled } d \times. \\
 & = \sum_{b_1} \sqrt{\frac{d_{b_1}}{d_{a_1} d_d}} \text{Diagram 2: Similar to Diagram 1, but with an additional edge } b_1 \text{ connecting } c_1 \text{ and } c_2. \\
 & = \sum_{b_1, b_4} \sqrt{\frac{d_{b_1}}{d_{a_1} d_d}} [F_{b_1}^{c_1 a_4 d}]_{a_1 b_4} \text{Diagram 3: Similar to Diagram 2, but with an additional edge } b_4 \text{ connecting } c_1 \text{ and } c_4. \\
 & = \sum_{b_1, b_2, b_3, b_4, b_5} \sqrt{\frac{d_{b_1}}{d_{a_1} d_d}} [F_{b_1}^{c_1 a_4 d}]_{a_1 b_4} [F_{b_4}^{c_4 a_3 d}]_{a_4 b_3} [F_{b_3}^{c_3 a_2 d}]_{a_3 b_2} [F_{b_2}^{c_2 a_1 d}]_{a_2 b_5} \text{Diagram 4: Similar to Diagram 3, but with an additional edge } b_2 \text{ connecting } c_2 \text{ and } c_3, \text{ and an additional edge } b_3 \text{ connecting } c_3 \text{ and } c_4. \\
 & = \prod_{i=1}^4 \sum_{b_i} [F_{b_i}^{c_i a_{i-1} d}]_{a_i b_{i-1}} \text{Diagram 5: A square with vertices labeled } c_1, c_2, c_3, c_4 \text{ and edges labeled } b_1, b_2, b_3, b_4. \text{ A cross inside is labeled } \times. \\
 & [F_d^{abc}]_{ef} = (-1)^{j_a + j_b + j_c + j_d} \sqrt{d_e d_f} \begin{Bmatrix} j_a & j_b & j_c \\ j_c & j_d & j_f \end{Bmatrix}
 \end{aligned}$$

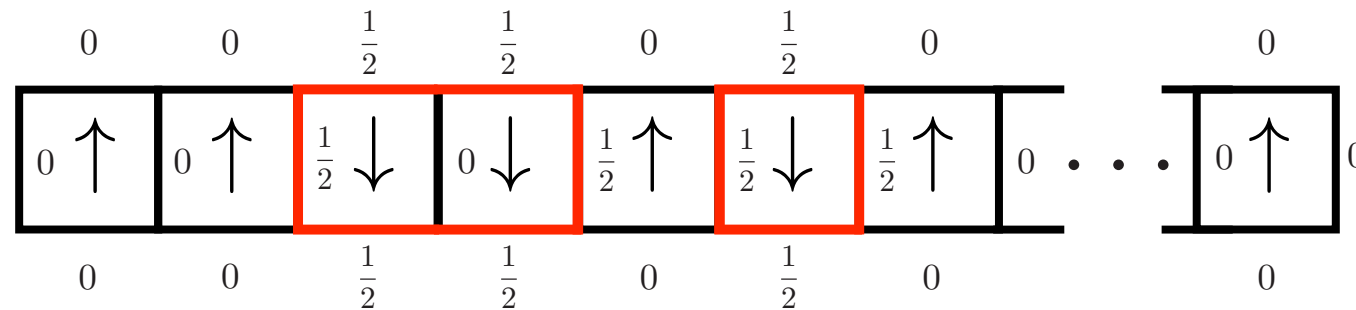
Wigner 6j symbol

# SU(2)<sub>1</sub> Yang-Mills model on a two-leg ladder

## Fusion rules



Plaquette chain = Qubit-chain



$N \times 1$  square lattice/ chain of plaquette



# SU(2)<sub>1</sub> Yang-Mills model on a two-leg ladder

## Fusion rules

$$\begin{array}{cc}
 \begin{array}{c} 0 \\ \bullet \\ \begin{array}{cc} 0 & 0 \end{array} \end{array} = |0, 0, 0\rangle, & \begin{array}{c} \frac{1}{2} \\ \bullet \\ \begin{array}{cc} 0 & \frac{1}{2} \end{array} \end{array} = |0, \frac{1}{2}, \frac{1}{2}\rangle, \\
 \begin{array}{c} \frac{1}{2} \\ \bullet \\ \begin{array}{cc} \frac{1}{2} & 0 \end{array} \end{array} = |\frac{1}{2}, \frac{1}{2}, 0\rangle, & \begin{array}{c} 0 \\ \bullet \\ \begin{array}{cc} \frac{1}{2} & \frac{1}{2} \end{array} \end{array} = |\frac{1}{2}, 0, \frac{1}{2}\rangle
 \end{array}$$

## F moves

The F moves are represented by two equations involving braiding of red and black lines:

$$\begin{array}{c} \text{Red} \rangle \text{Black} \rangle \end{array} = \begin{array}{c} \text{Red} \rangle \text{Red} \rangle \text{Black} \rangle \end{array}$$

$$\begin{array}{c} \text{Red} \rangle \text{Black} \langle \end{array} = - \begin{array}{c} \text{Red} \langle \text{Red} \rangle \text{Black} \rangle \end{array}$$

$$\begin{aligned}
\text{tr} U_{\frac{1}{2}} | \uparrow \uparrow \downarrow \rangle &= \text{I} \quad \frac{1}{\sqrt{d_0}} \quad \text{[Diagram I]} = \text{II} \quad \frac{1}{\sqrt{d_0}} \quad \text{[Diagram II]} \\
&= \text{III} \quad -\frac{1}{\sqrt{d_0}} \quad \text{[Diagram III]} = \text{IV} \quad -\frac{1}{\sqrt{d_0}} \quad \text{[Diagram IV]} \\
&= \text{V} \quad \frac{1}{\sqrt{d_0}} \quad \text{[Diagram V]} = \text{VI} \quad = - | \uparrow \downarrow \downarrow \rangle
\end{aligned}$$

Diagram I: A red loop encircling the top wire, with an 'x' inside. The bottom wire is a straight line.

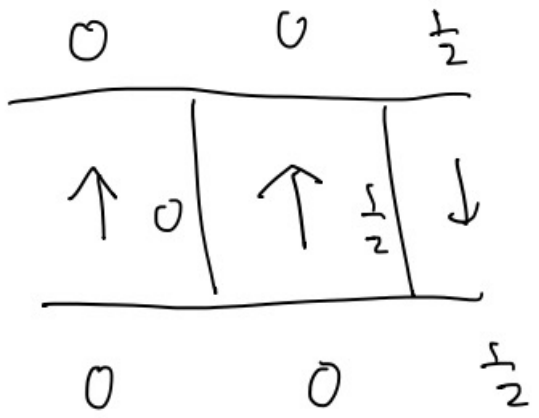
Diagram II: A red loop encircling both the top and bottom wires, with an 'x' inside.

Diagram III: A red loop encircling the top wire, with an 'x' inside. The bottom wire has a vertical line segment.

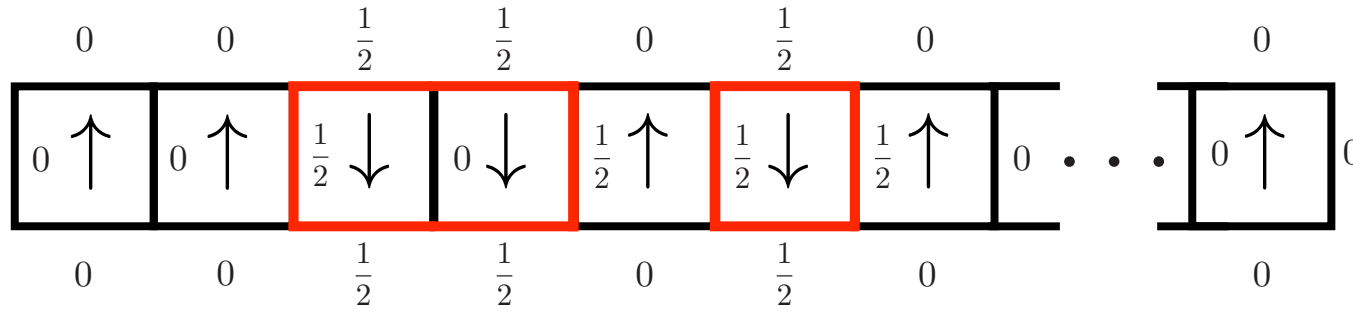
Diagram IV: A red loop encircling both the top and bottom wires, with an 'x' inside. The bottom wire has a vertical line segment.

Diagram V: A red loop encircling the bottom wire, with an 'x' inside. The top wire has a vertical line segment.

Diagram VI: A vertical line segment on the bottom wire, with an 'x' to its left.



# SU(2)<sub>1</sub> Yang-Mills model on a two-leg ladder



$$\text{tr}U_{\square}(i) | \uparrow\uparrow\uparrow \rangle = | \uparrow\downarrow\uparrow \rangle$$

$$\text{tr}U_{\square}(i) | \downarrow\downarrow\uparrow \rangle = - | \downarrow\uparrow\uparrow \rangle$$

$$\text{tr}U_{\square}(i) | \uparrow\downarrow\uparrow \rangle = | \uparrow\uparrow\uparrow \rangle$$

$$\text{tr}U_{\square}(i) | \downarrow\uparrow\uparrow \rangle = - | \downarrow\downarrow\uparrow \rangle$$

$$\text{tr}U_{\square}(i) | \uparrow\uparrow\downarrow \rangle = - | \uparrow\downarrow\downarrow \rangle$$

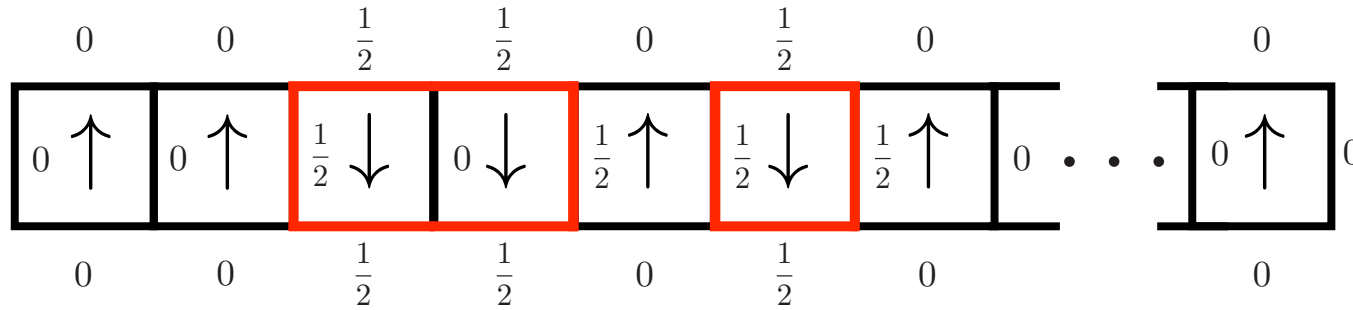
$$\text{tr}U_{\square}(i) | \downarrow\uparrow\downarrow \rangle = | \downarrow\downarrow\downarrow \rangle$$

$$\text{tr}U_{\square}(i) | \uparrow\downarrow\downarrow \rangle = - | \uparrow\uparrow\downarrow \rangle$$

$$\text{tr}U_{\square}(i) | \downarrow\downarrow\downarrow \rangle = | \downarrow\uparrow\downarrow \rangle$$

$$\text{tr}U_{\square}(i) = Z_{i-1} X_i Z_{i+1}$$

# SU(2)<sub>1</sub> Yang-Mills model on a two-leg ladder



$$H = \frac{c}{2} \sum_{n=1}^N (1 - Z_n) + \frac{c}{4} \sum_{n=1}^{N-1} (1 - Z_n Z_{n+1}) - K \sum_{n=1}^N Z_{n-1} X_n Z_{n+1}$$

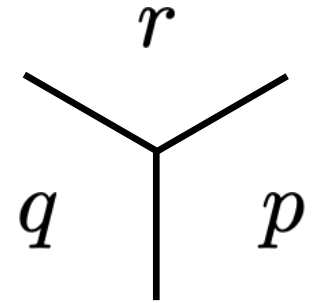
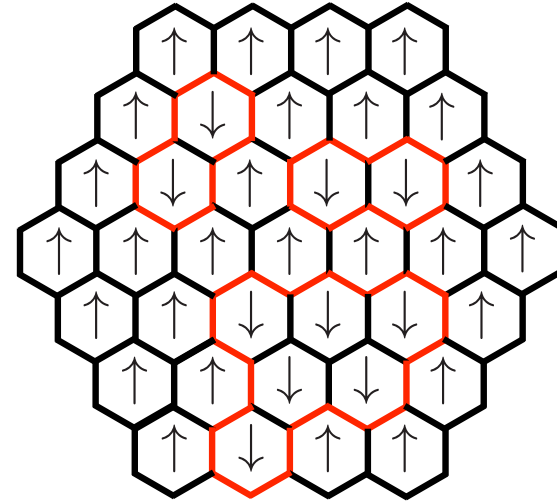
This model is unitary equivalent to the transverse-field Ising (TFI) model

$$U = e^{-i\frac{\pi}{4} \sum_n (-1)^n Z_n Z_{n+1}}$$

$$H = \frac{c}{2} \sum_{n=1}^N (1 - Z_n) + \frac{c}{4} \sum_{n=1}^{N-1} (1 - Z_n Z_{n+1}) - K \sum_{n=1}^N X_n$$

# SU(2)<sub>1</sub> Yang-Mills model on a honeycomb lattice

$$\begin{array}{l}
 \begin{array}{c} \uparrow \\ | \\ \bullet \\ / \quad \backslash \\ 0 \quad 0 \end{array} = |0, 0, 0\rangle, \quad \begin{array}{c} \uparrow \\ | \\ \bullet \\ / \quad \backslash \\ 0 \quad \frac{1}{2} \end{array} = |0, \frac{1}{2}, \frac{1}{2}\rangle, \\
 \begin{array}{c} \uparrow \\ | \\ \bullet \\ / \quad \backslash \\ \frac{1}{2} \quad 0 \end{array} = |\frac{1}{2}, \frac{1}{2}, 0\rangle, \quad \begin{array}{c} \uparrow \\ | \\ \bullet \\ / \quad \backslash \\ \frac{1}{2} \quad \frac{1}{2} \end{array} = |\frac{1}{2}, 0, \frac{1}{2}\rangle
 \end{array}$$



$$H = \frac{c}{4} \sum_{(n,m)} (1 - Z_n Z_m) - K \sum_p X_p \prod_{(q,r)} i^{\frac{1 - Z_q Z_r}{2}}$$

This model is unitary equivalent to the TFI model

$$U = \prod_{\langle pqr \rangle} e^{-i \frac{\pi}{24} (3Z_p Z_q Z_r - Z_p - Z_q - Z_r)}$$

$$H = \frac{c}{4} \sum_{(n,m)} (1 - Z_n Z_m) - K \sum_p X_p$$

What is the simplest LGT more complex than the TFI model?



$SU(3)_1$  on a two-leg ladder

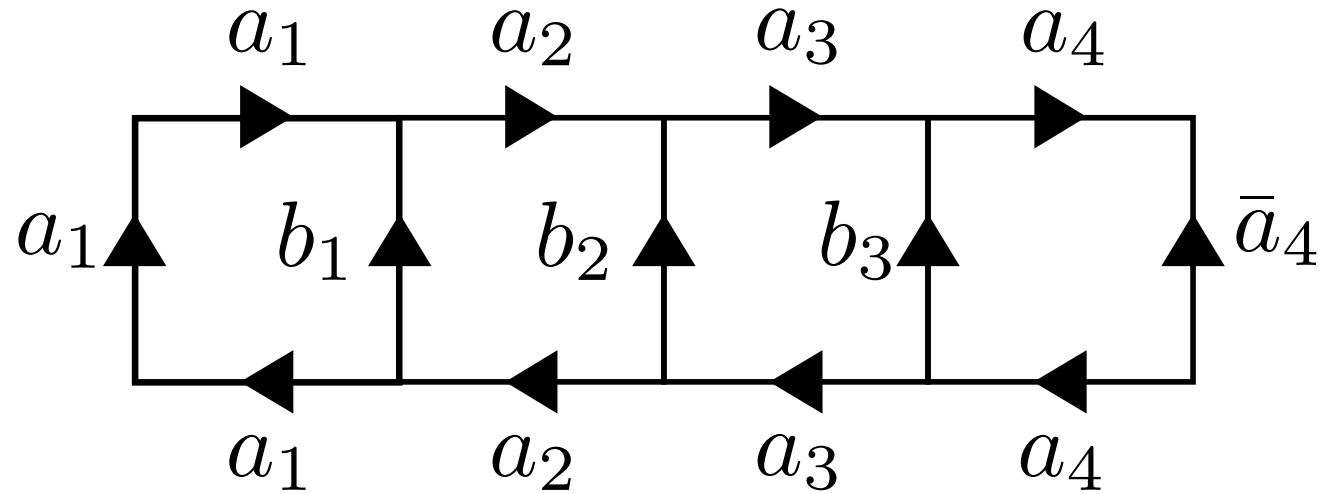
# SU(3)<sub>1</sub> Yang-Mills model on a two-leg ladder

Gauss law constraints

$$1 \times 1 = 1, \quad 1 \times 3 = 3 \times 1 = 3, \quad 1 \times \bar{3} = \bar{3} \times 1 = \bar{3},$$

$$3 \times 3 = \bar{3}, \quad 3 \times \bar{3} = 1, \quad \bar{3} \times \bar{3} = 3$$

Hilbert space

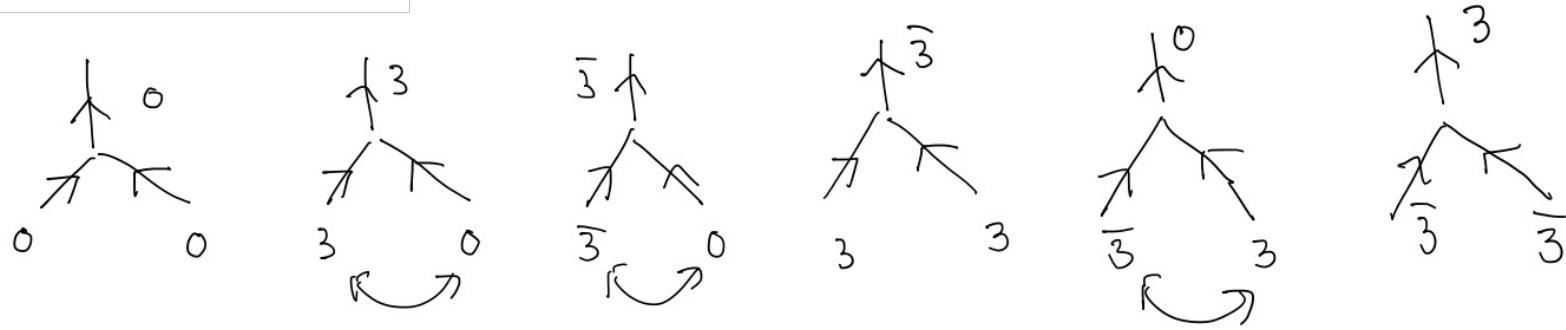


$$|\psi\rangle = \sum_{a_1, a_2, a_3, a_4 \in \{1, 3, \bar{3}\}} \psi(a_1, a_2, a_3, a_4) |a_1, a_2, a_3, a_4\rangle$$

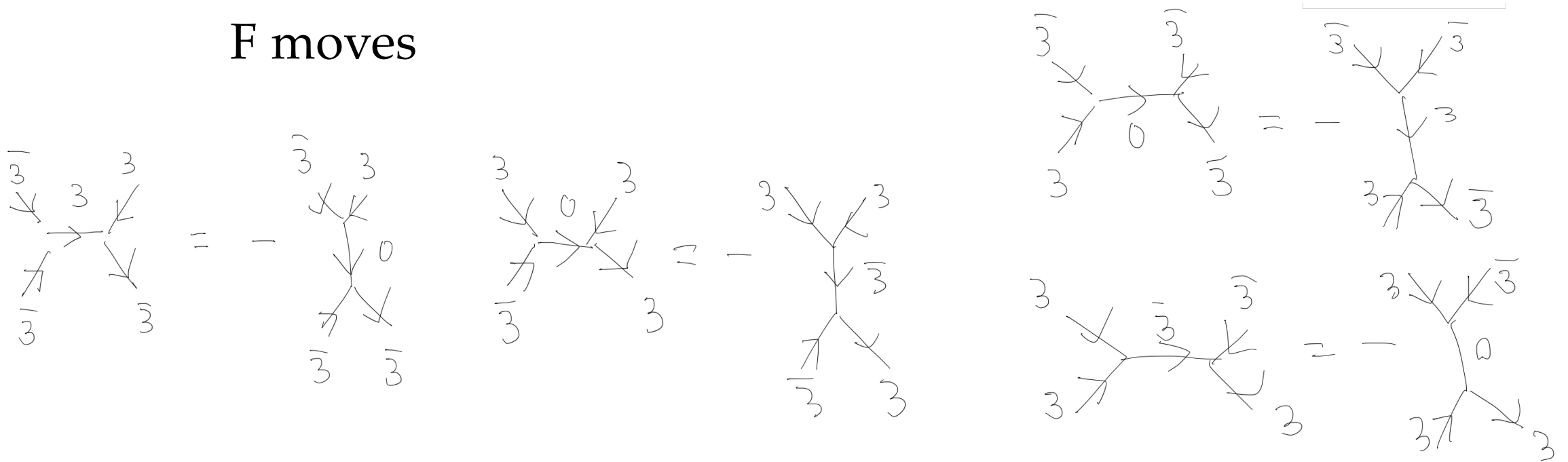
Qutrit chain

# SU(3)<sub>1</sub> Yang-Mills model on a two-leg ladder

## Fusion rules



## F moves





$$\text{tr}U_3|00\bar{3}\rangle =$$

I

II

III

IV

$$= -|03\bar{3}\rangle$$

$3 \times 3 \times 3$  patterns  $\rightarrow$  unitary transformation  $\rightarrow$  spin model

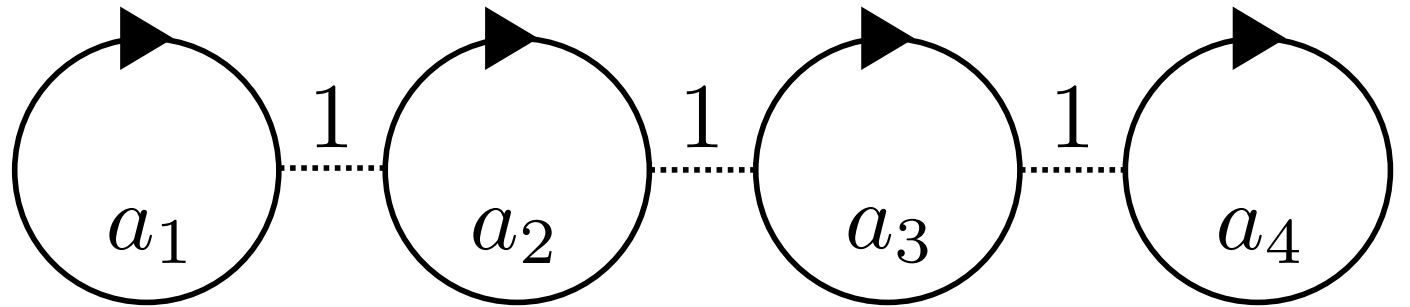
# $SU(3)_1$ Yang-Mills model on a two-leg ladder

Gauss law constraints

$$1 \times 1 = 1, \quad 1 \times 3 = 3 \times 1 = 3, \quad 1 \times \bar{3} = \bar{3} \times 1 = \bar{3}, \\ 3 \times 3 = \bar{3}, \quad 3 \times \bar{3} = 1, \quad \bar{3} \times \bar{3} = 3$$

Hilbert space

Dual basis = Plaquette basis



$$|\psi\rangle = \sum_{a_1, a_2, a_3, a_4 \in \{1, 3, \bar{3}\}} \psi(a_1, a_2, a_3, a_4) |a_1, a_2, a_3, a_4\rangle$$

**Qutrit chain**

# SU(3)<sub>1</sub> Yang-Mills model on a two-leg ladder

○ Hamiltonian of a qutrit chain

$$H_E = \frac{c}{2} \sum_{x=1}^N M(x) + \frac{c}{2} \sum_{x=1}^{N-1} M^r(x, x+1)$$

$$M = 2 \sum_{a=3, \bar{3}} |a\rangle\langle a| \quad M^r = \sum_{a=3, \bar{3}} (|a, 1\rangle\langle a, 1| + |1, a\rangle\langle 1, a| + |a, \bar{a}\rangle\langle a, \bar{a}|)$$

$$H_B = -\frac{K}{2} \sum_{x=1}^N [W(x) + W^\dagger(x)] \quad W = \begin{pmatrix} 0 & 0 & 1 \\ 1 & 0 & 0 \\ 0 & 1 & 0 \end{pmatrix}$$

# SU(3)<sub>1</sub> Yang-Mills model on a two-leg ladder

○ Mapping to qubit chain

$$|1\rangle \rightarrow |00\rangle \quad |3\rangle \rightarrow |01\rangle \quad |\bar{3}\rangle \rightarrow |10\rangle$$

$$\begin{aligned} M^{r(q)} &= \frac{1}{8}(3 + Z_1 + Z_2 + Z_3 + Z_4) \\ &+ \frac{1}{8}(-Z_1Z_2 + Z_2Z_3 - Z_3Z_4 + Z_1Z_4 - Z_1Z_3 - Z_2Z_4) \\ &+ \frac{1}{8}(-Z_1Z_2Z_3 - Z_2Z_3Z_4 - Z_1Z_2Z_4 - Z_1Z_3Z_4) \\ &- \frac{1}{8}Z_1Z_2Z_3Z_4 \end{aligned}$$

$$M_\phi = |11\rangle\langle 11|$$



Equivalent on logical space

$$\begin{aligned} \bar{M}^{r(q)} &= M^{r(q)} - 2M_\phi \otimes M_\phi + 2M_1 \otimes M_\phi + 2M_\phi \otimes M_1 \\ &= \frac{1}{2} + \frac{1}{4}(Z_1 + Z_2 + Z_3 + Z_4) - \frac{1}{2}(Z_1Z_3 + Z_2Z_4) - \frac{1}{4}(Z_2Z_3 + Z_1Z_4). \end{aligned}$$

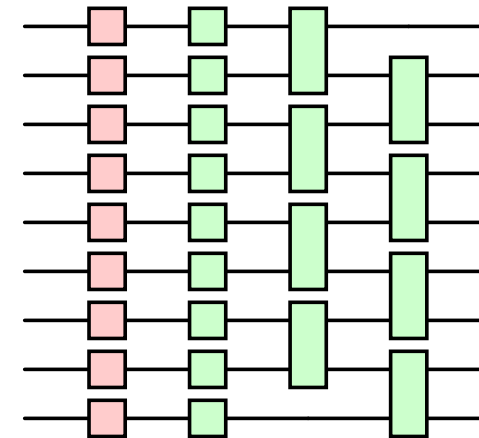
# SU(3)<sub>1</sub> Yang-Mills model on a two-leg ladder

○ 1<sup>st</sup> order Suzuki-Trotter decomposition

$$\mathcal{U}(T) = \left( e^{-idtH_E} e^{-idtH_B} \right)^M \quad W^{(q)} = \begin{pmatrix} 0 & 0 & 1 & 0 \\ 1 & 0 & 0 & 0 \\ 0 & 1 & 0 & 0 \\ 0 & 0 & 0 & 1 \end{pmatrix} \quad W^{(q)} = Q\Lambda Q^\dagger$$

$$e^{-idtH_E} = \prod_{x:\text{odd}} e^{-i\frac{1}{2}dt\bar{M}^{r(q)}(x,x+1)} \prod_{x:\text{even}} e^{-i\frac{1}{2}dt\bar{M}^{r(q)}(x,x+1)} \prod_x e^{-i\frac{1}{2}dtM^{(q)}(x)}$$

$$e^{-idtH_B} = \prod_x Q(x) e^{i\frac{K}{2}dt(\Lambda(x)+\Lambda^\dagger(x))} Q^\dagger(x)$$



$$\text{---} \square \text{---} = Q e^{i\frac{K}{2}dt(\Lambda+\Lambda^\dagger)} Q^\dagger$$

$$\text{---} \square \text{---} = e^{-i\frac{dt}{2}M^{(q)}}$$

$$\text{---} \square \text{---} = e^{-i\frac{dt}{2}\bar{M}^{r(q)}}$$

# Table of contents

- Why QC? → QC of QFT
- q-deformed Yang-Mills theory (Easy examples:  $SU(2)_1$  and  $SU(3)_1$ )
- Why Floquet systems?
- Experimental results
- Summary

Artificial tasks  
(Random circuits)

Google '19  
Zuchongzhi '21  
Quantinuum '24

What can we do?

Important tasks

Prime factoring  
Quantum chemistry  
Cond-mat physics  
⋮



Time



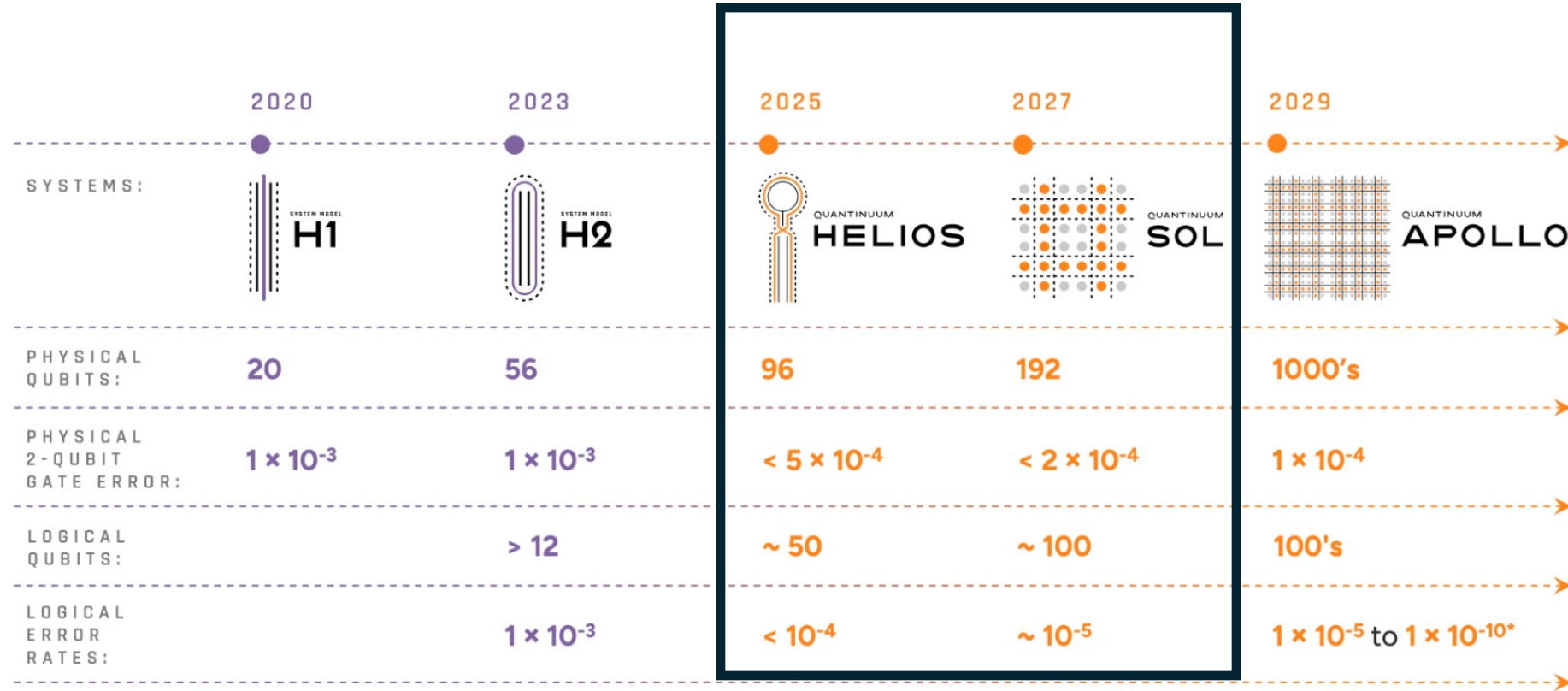
Deal with noises



Fault-tolerant QC

# What can we do?

## Development roadmap



© 2024 Quantinuum. All Rights Reserved.

\*analysis based on recent literature in new, novel error correcting codes predict that error could be as low as  $1E-10$  in Apollo (ref: arXiv:2403.16054, arXiv:2308.07915)

physical qubits are more useful than logical qubits



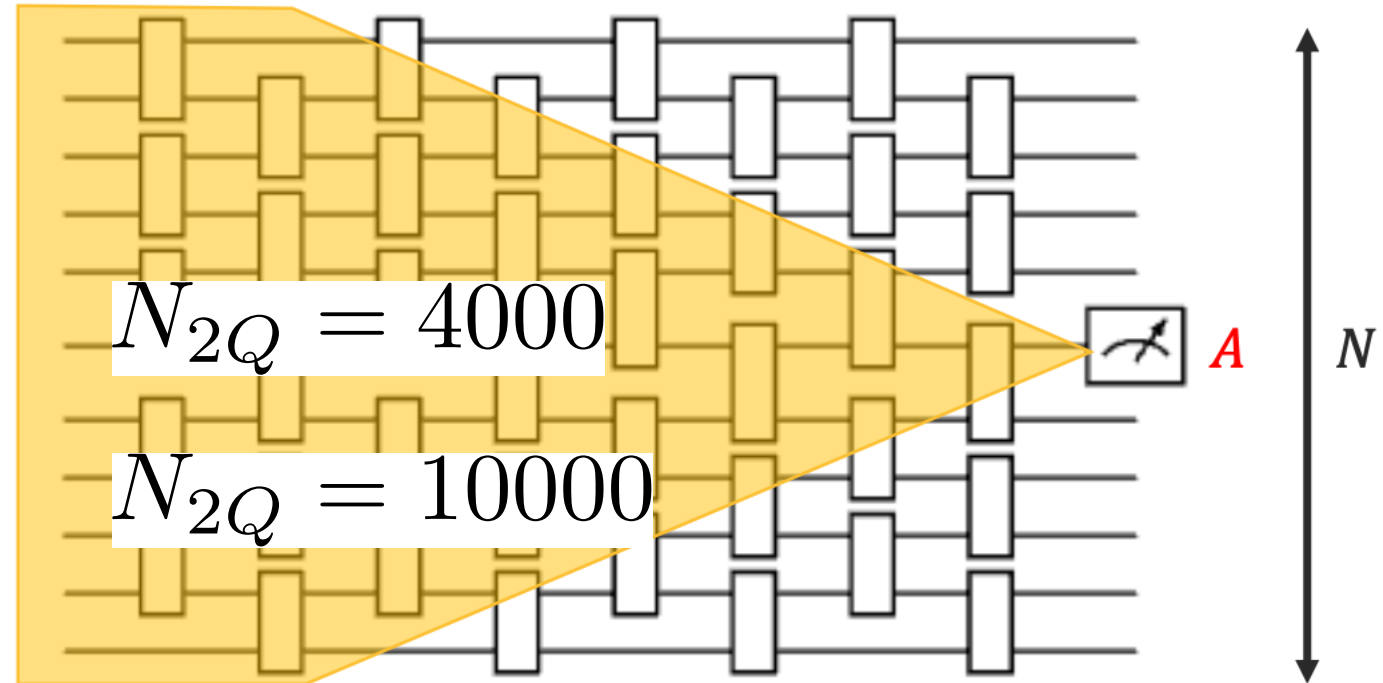
# What can we do?

○ global depolarizing model  $\langle \hat{O} \rangle_{\text{noisy}} = f \langle \hat{O} \rangle_{\text{ideal}}$

$$f = (1 - p)^{N_{2Q}} = 0.135$$

$$p = 5 \times 10^{-4}$$

$$p = 2 \times 10^{-4}$$



$$N = 100, \quad dt = 0.1, \quad t = 10, \quad N_{2Q} \sim 10000$$

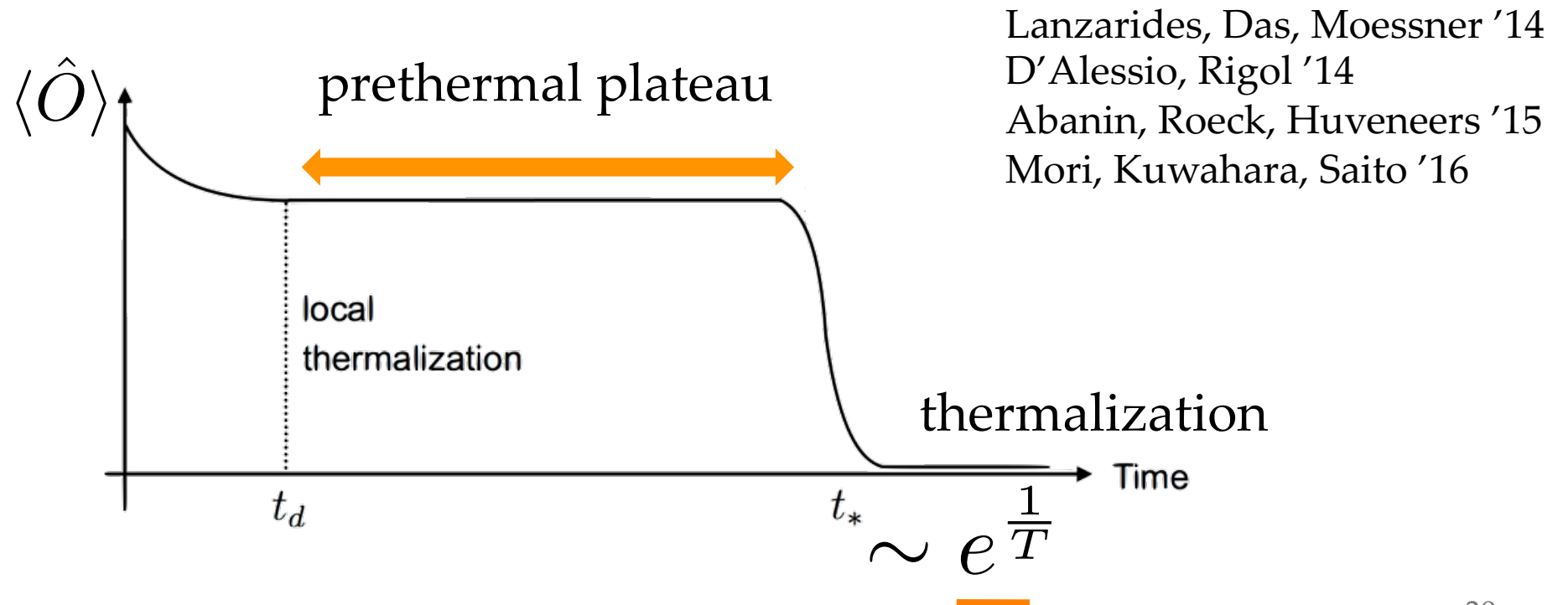
Hamiltonian simulation of LGTs is challenging in the NISQ era

# Floquet dynamics

- Time evolution with a time-dependent Hamiltonian

$$i\partial_t|\Psi\rangle = H|\Psi\rangle \quad H(t+T) = H(t)$$

driven system  $\rightarrow$  heat up to infinite temperature



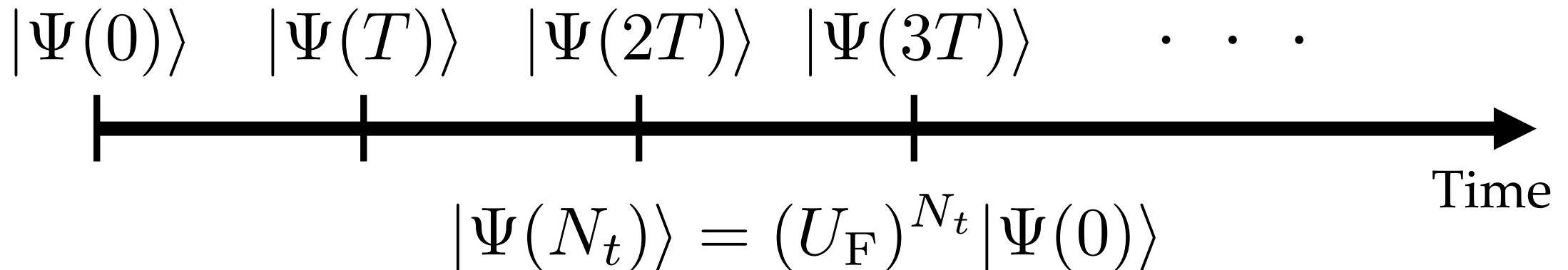
# Trotter dynamics

○ Trotter dynamics can be understood as Floquet dynamics

$$U_F = e^{-iH_1 dt} e^{-iH_2 dt} \quad H(t) = \begin{cases} H_1 & t \in [0, T/2), \\ H_2 & t \in [T/2, T) \end{cases}$$

$$dt = \frac{T}{2}$$

$$i\partial_t |\Psi\rangle = H |\Psi\rangle \quad H(t+T) = H(t)$$



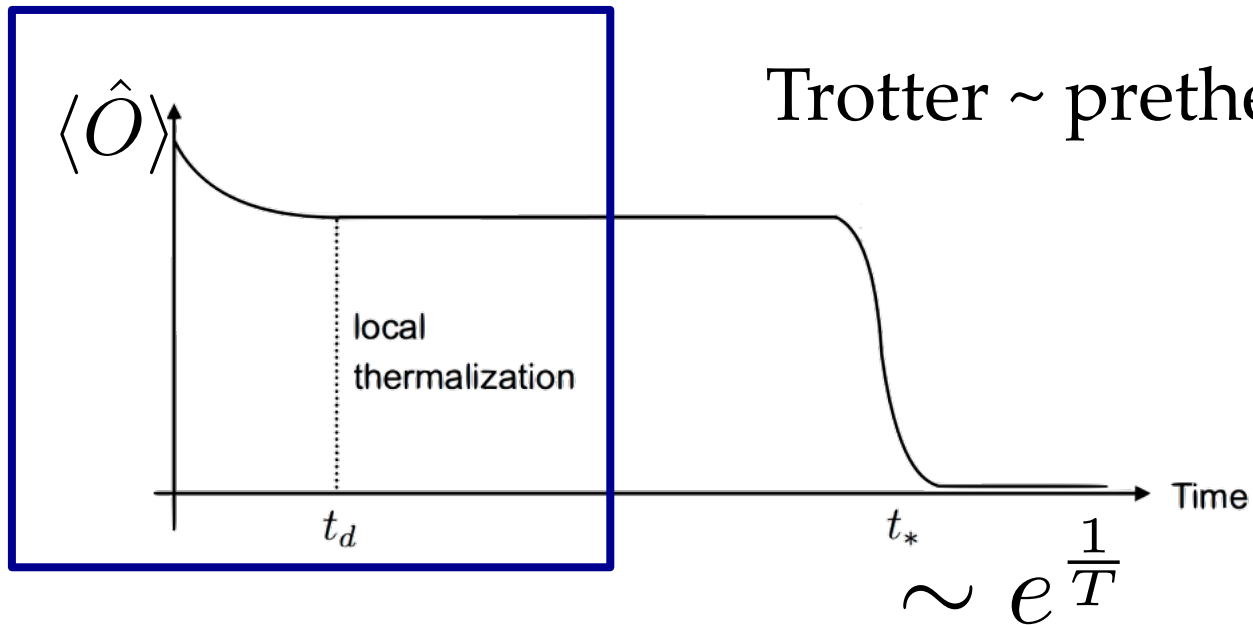
# Trotter dynamics

## ○ Trotter transition

Heyl, Hauke, Zoller '18

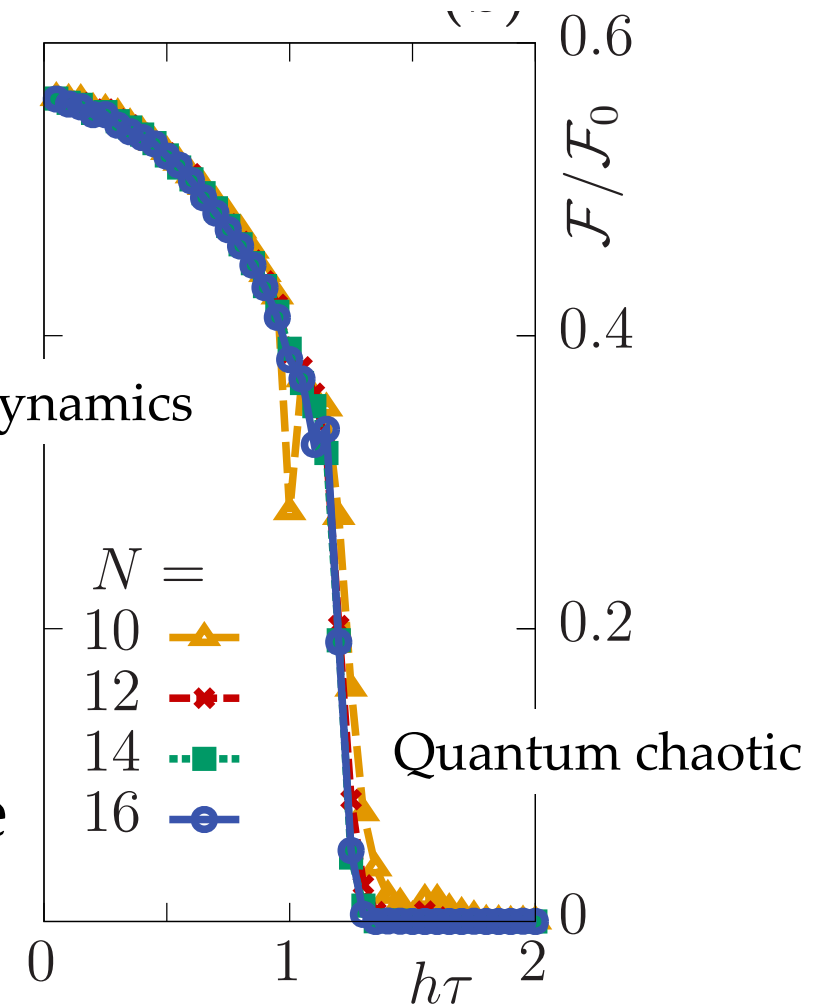
Varnier, Bertini, Giudici, Piroli '23

Trotter error is under control if  $dt < dt_c$



Trotter dynamics

OTOC



prethermalizaion dynamics  
is feasible to NISQ devices

# Trotter dynamics as Floquet dynamics

○ Feasibility of information scrambling on the present best fidelity hardware

Next talk!

Ion traps: Kazuhiro Seki, Yuta Kikuchi, Tomoya Hayata, Seiji Yunoki, 2405.07613 [quant-ph]

○ Prethermalization dynamics with many qubits

Superconducting qubits:

1+1d  $Z_2$ : Tomoya Hayata, Kazuhiro Seki, Arata Yamamoto, arXiv:2408.10079 [hep-lat]

$SU(3)_1$ : Tomoya Hayata, Yoshimasa Hidaka, 2409.20263 [hep-lat]

# Table of contents

- Why QC? → QC of QFT
- q-deformed Yang-Mills theory (Easy examples:  $SU(2)_1$  and  $SU(3)_1$ )
- Why Floquet systems?
- Experimental results
- Summary

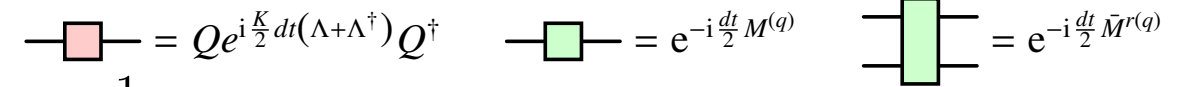
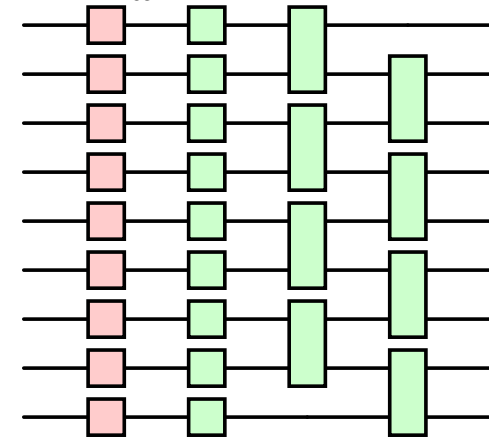
# SU(3)<sub>1</sub> Yang-Mills model on a two-leg ladder

○ 1<sup>st</sup> order Suzuki-Trotter decomposition

$$\mathcal{U}(T) = \left( e^{-idtH_E} e^{-idtH_B} \right)^M \quad W^{(q)} = \begin{pmatrix} 0 & 0 & 1 & 0 \\ 1 & 0 & 0 & 0 \\ 0 & 1 & 0 & 0 \\ 0 & 0 & 0 & 1 \end{pmatrix} \quad W^{(q)} = Q\Lambda Q^\dagger$$

$$e^{-idtH_E} = \prod_{x:\text{odd}} e^{-i\frac{1}{2}dt\bar{M}^{r(q)}(x,x+1)} \prod_{x:\text{even}} e^{-i\frac{1}{2}dt\bar{M}^{r(q)}(x,x+1)} \prod_x e^{-i\frac{1}{2}dtM^{(q)}(x)}$$

$$e^{-idtH_B} = \prod_x Q(x) e^{i\frac{K}{2}dt(\Lambda(x)+\Lambda^\dagger(x))} Q^\dagger(x)$$



$$\bar{M}^{r(q)} = \frac{1}{2} + \frac{1}{4}(Z_1 + Z_2 + Z_3 + Z_4) - \frac{1}{2}(Z_1Z_3 + Z_2Z_4) - \frac{1}{4}(Z_2Z_3 + Z_1Z_4)$$

# QC summary

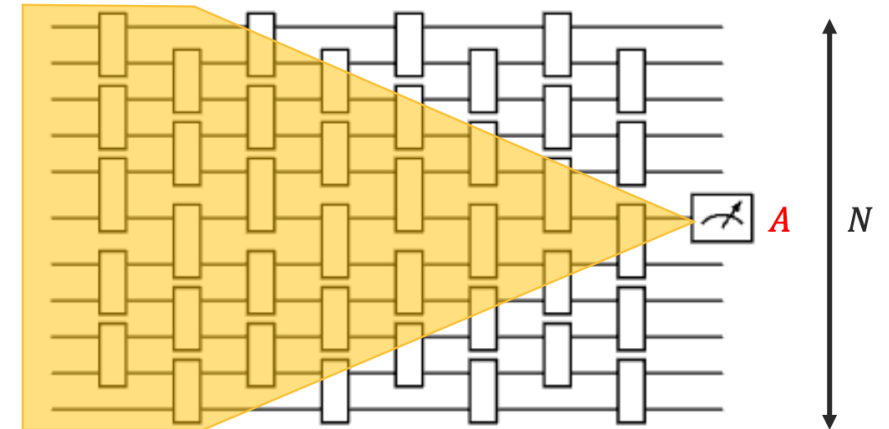
○  $dt = 2\pi$  (We can reduce 2Q gates)/ Change  $K$

○ `ibm_fez` is used

○ 10,000 shot is used

○ Pauli twirling is enabled/ DD is disabled

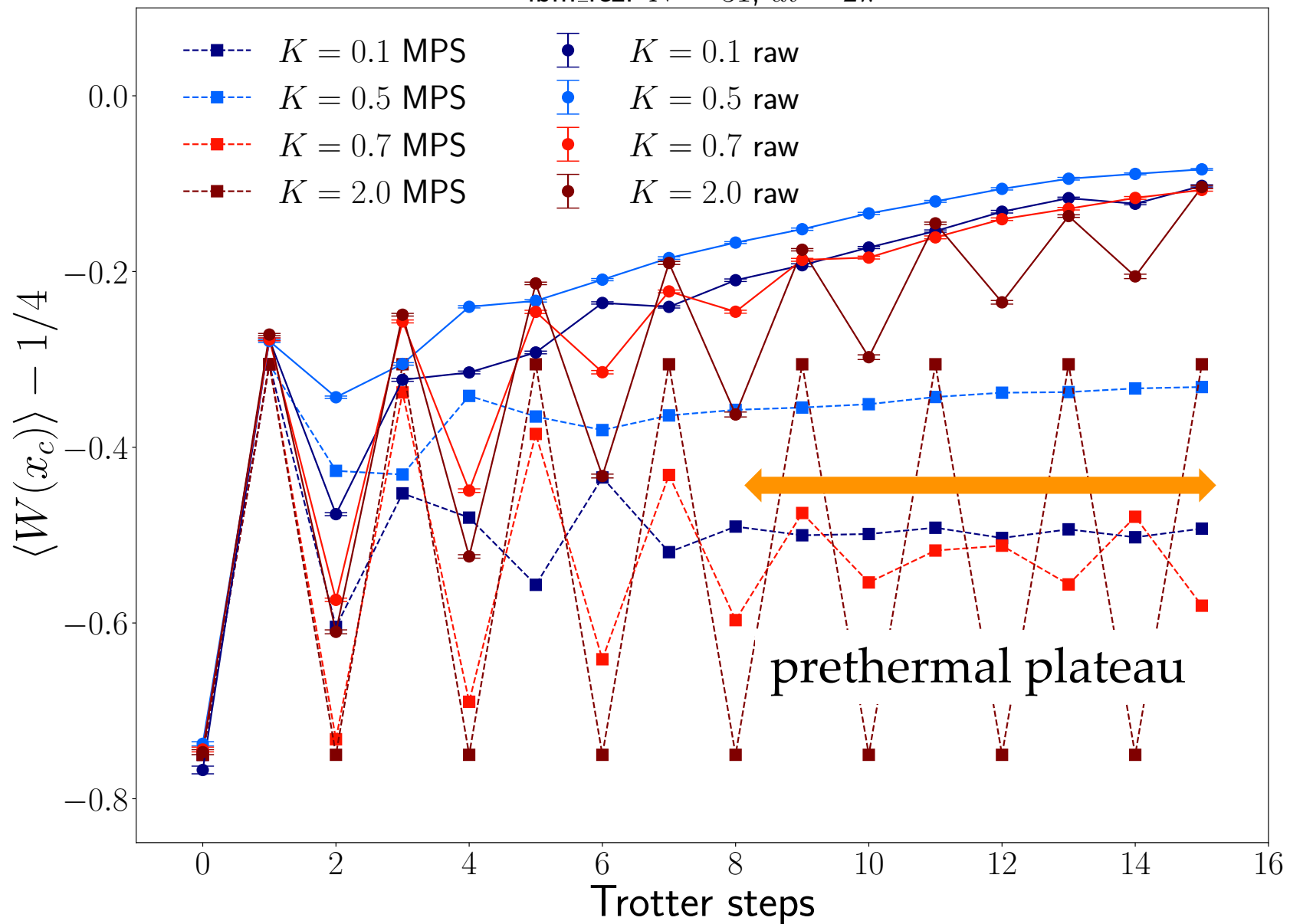
○ Unnecessary gates outside of the causal cone are removed





# Experimental results (raw data)

ibm\_fez:  $N = 31$ ,  $dt = 2\pi$



Error mitigation is necessary to do quantitative analysis

# Quantum error mitigation (“Gauss’ laws”)

- global depolarizing channel

$$\langle \hat{O} \rangle_{\text{raw}} = f \langle \hat{O} \rangle_{\text{ideal}} + \frac{1-f}{2^{3N-1}} \text{Tr} \hat{O}$$

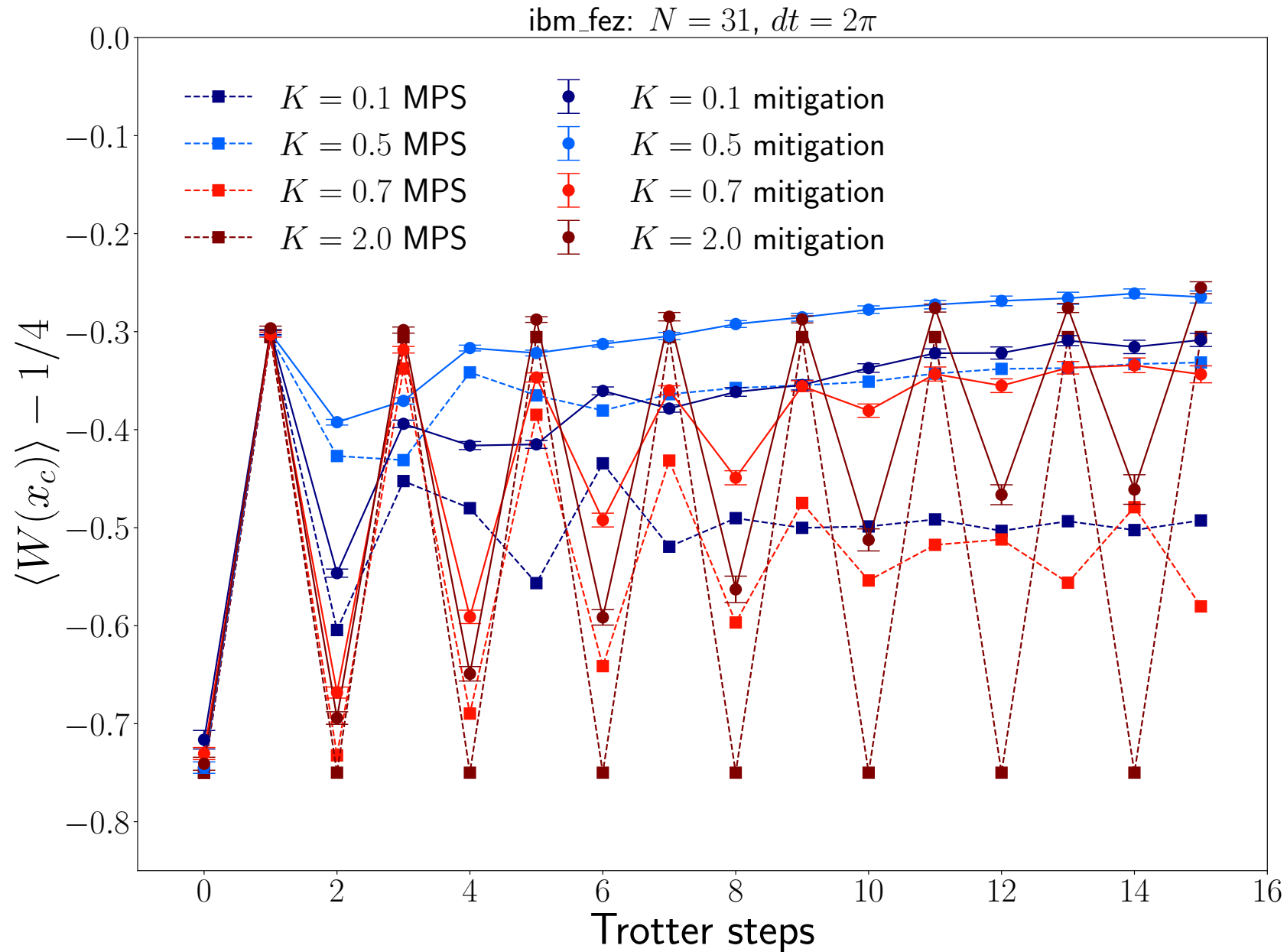
- estimate  $f$  by measuring  $M_\phi = |11\rangle\langle 11|$

$$\langle M_\phi \rangle_{\text{ideal}} = 0 \quad \longrightarrow \quad \langle M_\phi \rangle_{\text{raw}} = \frac{1-f}{4}$$

- rescale observables by

$$\langle O(x) \rangle_{\text{mit}} = \frac{\langle O(x) \rangle_{\text{raw}}}{1 - 4 \langle M_\phi(x) \rangle_{\text{raw}}}$$

# Experimental results (“Gauss’s law”)



Improved but not  
better than we expected

# Quantum error mitigation (ODR)

- global depolarizing channel

$$\langle \hat{O} \rangle_{\text{raw}} = f \langle \hat{O} \rangle_{\text{ideal}} + \frac{1-f}{2^{3N-1}} \text{Tr} \hat{O}$$

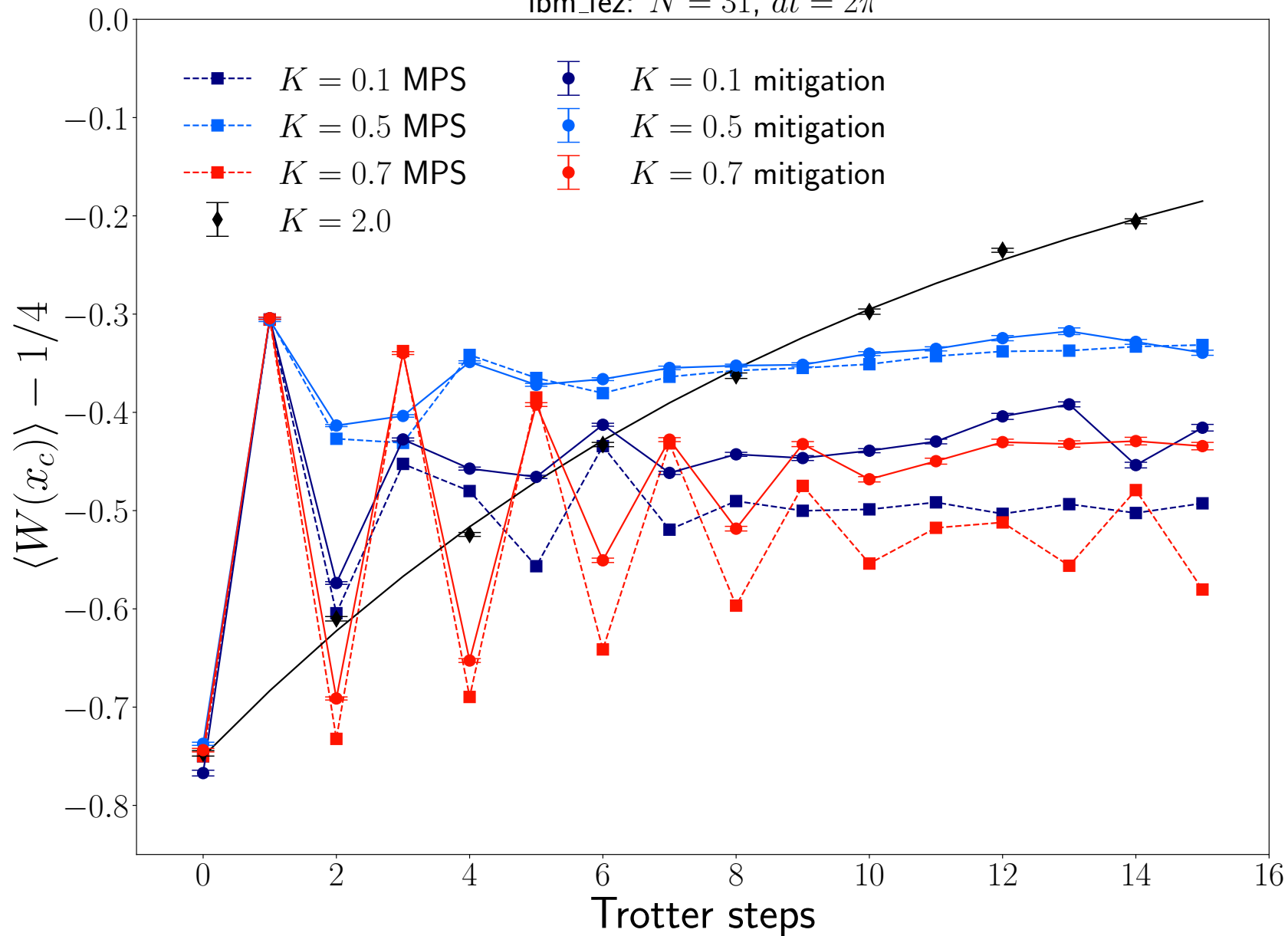
- run the same circuit with the “solvable” parameter

- rescale observables by

$$\langle \hat{O} \rangle_{\text{mit}} = \frac{\langle \hat{O} \rangle_{\text{raw}}}{f}$$

# Experimental results (ODR)

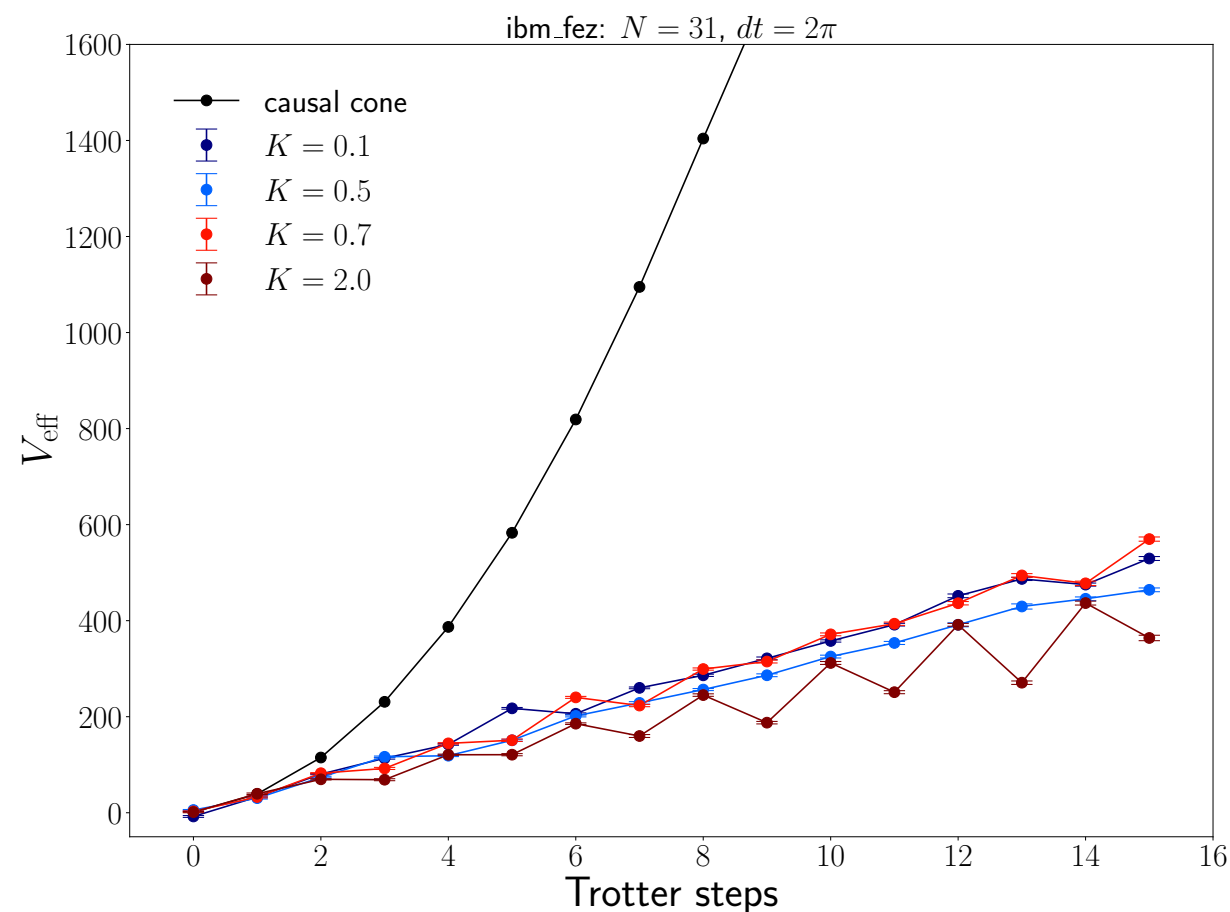
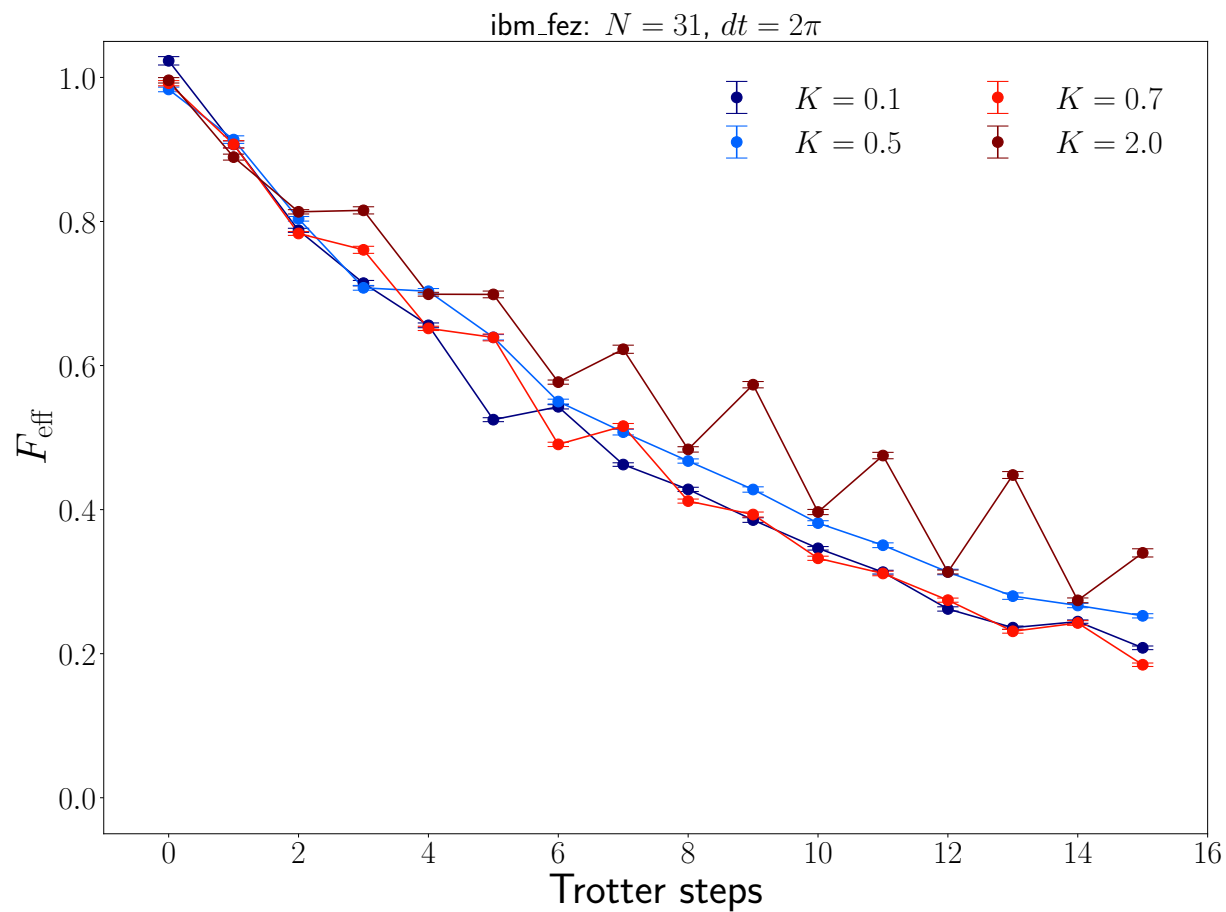
ibm\_fez:  $N = 31$ ,  $dt = 2\pi$



Successful in running  
Floquet circuit with  $N_t > 10$

ODR may be the first choice  
if ZNE is not applicable

# Fidelity and circuit volume



Estimate 2Q gate involved to compute the expectation value from the fidelity decay

# Summary

- QC for QCD is anticipated but challenging
- Quantum simulation of Floquet circuits in near future devices is interesting and may be useful for showing quantum advantage
- Lattice gauge theories have complex Hamiltonians and may provide good playgrounds for testing the capability of QCs

Thank you!